



Journal of Mining and Environment (JME)

journal homepage: [www.jme.shahroodut.ac.ir](http://www.jme.shahroodut.ac.ir)



## Sensitivity Analysis of Stress and Cracking in Rock Mass Blasting using Numerical Modelling

Mohammad Ali Chamanzad and Majid Nikkhah\*

Faculty of Mining, Petroleum & Geophysics Engineering, Shahrood university of technology, Shahrood, Iran

### Article Info

Received 31 August 2020

Received in Revised form 21 September 2020

Accepted 21 September 2020

Published online 03 October 2020

DOI:10.22044/jme.2020.10033.1939

### Keywords

Blasting

Distinct element method

Numerical modelling

Discontinuity

Rock mass

### Abstract

Drilling and blasting have numerous applications in the civil and mining engineering. Due to the two major components of rock masses, namely the intact rock matrix and the discontinuities, their behavior is a complicated process to be analyzed. The purpose of this work is to investigate the effects of the geomechanical and geometrical parameters of rock and discontinuities on the rock mass blasting using the UDEC software. To this end, a 2D distinct element code (DEM) code is used to simulate the stress distribution around three blast holes in some points and propagation of the radial cracks caused by blasting. The critical parameters analyzed for this aim include the normal stiffness (JKN) and shear stiffness (JKS), spacing, angle and persistence of joint, shear and bulk modulus, density of rock, and borehole spacing. The results obtained show that the joint parameters and rock modulus have very significant effects, while the rock density has less a effect on the rock mass blasting. Also the stress level has a direct relationship with JKN, JKS, bulk modulus, and the shear modulus has an inverse relationship with the rock density. Moreover, the stress variation in terms of spacing and joint angle indicates sinusoidal and repetitive changes with the place of target point with respect to the blast hole and joint set. Also with a decrease in the JKN and JKS values, the radial cracked and plastic zones around a blast hole show more development. With increase in the joint persistence, the plastic zones decrease around a blast hole.

### 1. Introduction

Rock mass, as an important material in rock engineering, is constructed with intact rock and discontinuities. As the rock mass is not continuous and the behavior of the discontinuities such as joints, faults, and bedding is so complicated, the behavior of rock mass has been considered to be controlled by the discontinuity behavior. Demolition of hard rocks using blasting usually involves the drilling of blast holes, placement of an explosive charge, and stemming before detonation. When the explosive is detonated, an extremely high-pressure pulse is generated, which is transmitted into the rock mass adjacent to the blast holes, producing a dilatational wave that propagates away from the charge. This may cause a damage to the rock, and when the compressive stress wave reaches a free face or fissure (non-transmission), it will be

reflected and converted into a tensile wave, which may produce tensile cracking or cause spalling of surficial slabs if the tensile strength of the rock is exceeded [1–3].

The control of some phenomena such as the ground vibration, fly rock, back break, and unfavorable displacement produce an extension of the undesirable cracks, and the extended crushed zone is so important in the blasting operation [4, 5]. By paying attention to the application of blast operation that is used in the mining and civil industries, the control of blasting, which plays an important role in the unsafety of the mining and civil activities, should be attended [1]. A lot of research works, from 1950 until now, by presenting the mathematical, experimental, and analytical

✉ Corresponding author: [m.nikkhah@shahroodut.ac.ir](mailto:m.nikkhah@shahroodut.ac.ir) (M. Nikkhah).

models, have tried to control or predict the blasting consequences [6–8].

Some researchers believe that cracking is mainly caused by the incident dilatational wave and any reflected waves, while other investigators have considered the action of the compressed gases forcing its way through the cracks from the blast hole more important. Until recently, it is generally agreed that both the stress wave and gas pressure loadings play an important role in the process of rock fracture and fragmentation. Our understanding of the blasting process is far from thorough as both the explosive and the rock are complex materials [2, 3]. At the same time, it is necessary to explore the fracture and fragmentation processes through numerical tools in order to obtain a better understanding of the underlying mechanism. A numerical approach has been developed to simulate multiple fracture propagation due to the stress waves and detonation gas [9].

For the suggestions and control of the blasting, which are placed and happen around the blast hole, different methods have been presented. In 1963, Ash, for controlling the unfavorable ingredients and improving the favorable result of blasting, has presented the experimental models. In these models, using the relative density of rock and relative power of explosion material, the radius of the breakage zone has been obtained as a coefficient of blast hole radius [10]. In 1973, Drukovanyi et al. have used the Illiyushin material behavior theory, presented in 1971, to analyze the crack distribution around a blast hole with the assumption that the rock medium has been considered continuum and explosion of explosive material in rock medium has been considered as a plain strain [11]. Insistence in the use of Illiyushin material behavior theory is the weak point of these models. In 1973, evaluation of the crush zone extension around a single blast hole has been presented by Vovk et al. They used some experimental tests for predicting the crush zone around a blast hole and also presented an equation [12].

In 1993, Szuladzinski presented an experimental equation in order to predict the radius of the crush zone around a blast hole with respect to the hydrodynamical theory of explosion in rock [13]. The effective energy of the explosive material was used in this model, in which the precision of this parameter was low. In 1999, Kanchibotla et al. have expressed that the radius of the crush zone around a hole correlates to the radius of hole, explosion pressure, and uniaxial compressive strength of rock mass, and with the use of these parameters, they presented an experimental equation for prediction of

the crush zone radius [14]. It is necessary to notice that the value of the crush zone radius, which is calculated from the Szuladzinski, Djordjevic and, Kanchibotla equations, is more than the real value obtained from the blast operation. In 2003, Esen et al. presented a parameter called the crush zone ratio (CZI) for predicting the radius of the crush zone around a blast hole as a result of 92 experimental tests. In this research work a negative exponential equation based on the crush zone ratio (CZI) is presented, and the result of that is compared with the experimental equations [15]. In 2010, the result of concrete block explosion with the use of ANFO was compared with the experimental equations. In this analysis, the radial crack zone and the crush zone around a blast hole were calculated using the experimental equations, and then the result of that was compared with the result obtained from the concrete block explosion [16]. In 2009, the result of the Iverson et al. research work expressed that in the zones with more explosive materials, the crush zone and the radial cracked zone were more than the other zones with low explosive materials. Between the experimental models that Iverson et al. analyzed, the Ash experimental model is more realistic than the others in the prediction of the damaged zone around a blast hole.

The simulation results gave a better understanding of the importance of discontinuities in the wave energy absorption [17]. The influences of the loading and boundary conditions on the rock fracture pattern were extensively investigated by Ma & An in 2008 [18]. The presence of the discontinuities has a significant influence on the responses of the rock mass to either static or dynamic loading renders and the numerical simulations are more complicated [19]. A 2D dynamic commercial code was employed by Sharafisafa et al. in 2014 to study the pre-splitting blast method. The histories of maximum stresses at halfway between two blastholes in 0.2 ms have been examined for blast hole spacing, blast loading, blasthole diameter, and joint pattern [20]. Kulatilake et al. have performed a numerical modelling with a 3D distinct element code (3DEC) in order to analyze the performance of cavern walls in terms of displacement and to compute peak particle velocities (PPVs) both around the cavern periphery and at the surface of the models [21].

It is well-recognized that the properties of a rock mass are determined by the properties of the intact rock and the discontinuities such as the joint structures and faults. In this work, the influence of the geomechanical and geometrical parameters on stress level and radial crack extension of mudstone,

which is located in the Gotvand Dam project, was studied using the UDEC software. To this end, a 2D distinct element code (DEM) was used to simulate the stress distribution around three blast holes in some points and propagation of radial cracks caused by blasting in one hole. The critical parameters analyzed for this aim included the normal stiffness (JKN) and shear stiffness (JKS), spacing, angle and persistence of joint, shear and bulk modulus, density of rock, and borehole spacing. It was found that the stress level had a direct relationship with the JKN, JKS, and bulk modulus, and the shear modulus had an inverse relationship with the rock density. Moreover, stress variation in terms of spacing and joint angle indicates sinusoidal and repetitive changes with the place of target point with respect to the blast hole and joint set. Also with a decrease in the JKN and JKS values, the radial cracked and plastic zones around a blast hole showed more development with increase in the joint persistence, and the plastic zones decreased around a blast hole.

**2. Numerical modelling**

In this analysis, for simulation of the blasting process, the numerical analysis was conducted using the UDEC software. The simulation rock mass, which consisted of three blast holes (for stress analysis) and one blast hole (for the cracked zone) was analyzed. This simulation consisted of some stages such as the explosion model define and choosing an appropriate model for the behavior of rock mass and discontinuities. Defining the medium of blast hole, boundary condition, static and equilibrium condition analysis, viscous boundary conditions for dynamic simulation, import dynamic loading into the model, dynamic analysis classification, and results were carried out.

It is well-known that the existence of discontinuities in rock masses is a challenging task. UDEC has been specially developed to model the discontinuous problems. It can accommodate a large number of discontinuities, and permits the

modelling system to undergo larger geometrical changes through the use of a contact updating scheme. In UDEC, the deformation of a fractured rock mass consists of the elastic/plastic deformation of blocks of intact rock together with the displacements along and across the fractures. The motion of block is characterized by the Newton’s second law of motion, which is expressed in the central finite difference form versus time. The calculations are performed over one time step in an explicit time-marching algorithm. For the deformable blocks, a numerical integration of the differential equation of motion is used to determine the incremental displacements at the grid points of the triangular constant strain element within the blocks [22–24]. The incremental displacements are then used to calculate the new stresses within the element through an appropriate constitutive equation. The amount of normal and tangential displacement between two adjacent blocks can be determined directly from the block geometry and the translation and rotation of the centroid of each block. The intact rock blocks were assumed to be perfectly elastic in the present work. As for the joint behavior model, many types of constitutive laws may be contemplated [22–24].

The Jones-Wilkens-Lee (JWL) equation of state was used to model the pressure generated by the expansion of the detonation product of the chemical explosive. It has been widely used in engineering calculations, and can be written as [23, 24]:

$$P = C_1 \left(1 - \frac{\omega}{r_1 V}\right) e^{-r_1 V} + C_2 \left(1 - \frac{\omega}{r_2 V}\right) e^{-r_2 V} + \frac{\omega e}{V} \tag{1}$$

where  $C_1$ ,  $r_1$ ,  $C_2$ , and  $r_2$  are the material constants,  $P$  is the pressure,  $V$  is the specific volume, and  $e$  is the specific energy with an initial value of  $e_0$ . The JWL parameters for the explosive used (TNT) in this work are presented in Table 1.

**Table 1. JWL parameters for TNT explosive [22].**

Density (kg/m <sup>3</sup> )	C <sub>1</sub> (Gpa)	C <sub>2</sub> (Gpa)	R <sub>1</sub>	R <sub>2</sub>
1640	373.78	3.23	4.15	0.95

There are many examples of the velocity of blast loading that are imported into the model [22]. The results of the imported velocity in the UDEC software in this research work are shown in Figure 1.

The damping in the numerical simulations should attempt to reproduce the energy loss in the system when subjected to dynamic loading. The Rayleigh damping is commonly used to provide damping, which is approximately frequency-independent over a restricted range of frequencies. In order to

find the principal frequency of the input velocity history (refer to Figure 1), a spectral analysis should be made before the simulations. As it can be seen in

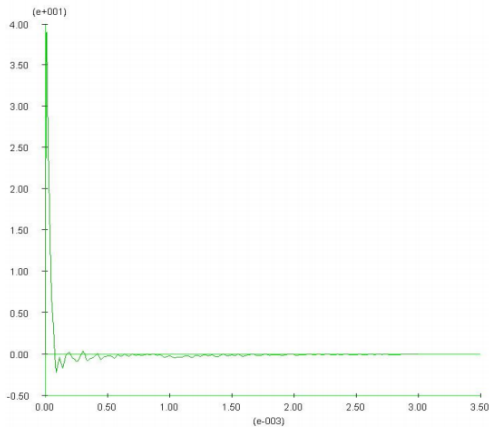


**Figure 1. Explosion time history of dynamic loading imported UDEC software.**

The damping parameters are very important for the UDEC dynamic analyses. They are also related to the maximum edge length of the triangle-shaped finite-difference zones of UDEC modelling. Some research works show that for an accurate representation of wave transmission through a model, the spatial element size ( $\nabla l$ ) must be smaller than approximately one-tenth to one-eighth of the wavelength  $\lambda$  associated with the highest frequency component that contains an appreciable energy [10].

$$\Delta l \leq \left( \frac{1}{10} - \frac{1}{8} \right) \lambda \quad (2)$$

Again, in order to satisfy the comparability, each block in the UDEC modelling was sub-divided into

Figure 2, the principal frequency of the blast wave is obtained via a fast Fourier transform algorithm.

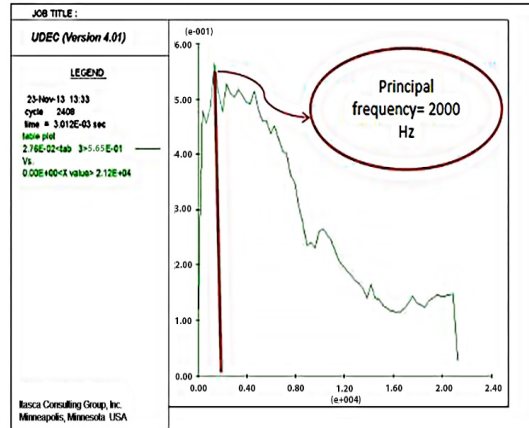


**Figure 2. Power spectrum of the input velocity–time history.**

the constant-strain finite-difference triangular zones. Preliminary analyses show that the adoption of a zone size of 0.14 m for the present problem is small enough to allow the waves to propagate accurately at the input frequency without distortion. Another important item in the dynamic analysis is the reproduction of frequency-independent damping of materials at the correct level. For soil and rock, the natural damping commonly falls in the range of 2.0–5.0% of the critical value [10].

The geomechanical properties of the Gotvand dam site project mudstone are shown in Table 2, and the input geomechanical properties of the joints are depicted in Table 3.

**Table 2. Geomechanical parameters of Gotvand sie mudstone.**

Density (kg/m <sup>3</sup> )	Bulk modulus (GPa)	Shear modulus (GPa)	Cohesion (Mpa)	Friction angle (°)
2370	8.3	6.2	4.2	33

**Table 3. Geomechanical properties of joints.**

Normal stiffness (GPa/m)	Shear stiffness (GPa/m)	Cohesion (Mpa)	Friction angle (°)	Angle with the x-axis (°)
8e9	1.06	0.15	30	120

Also the geometry and boundary conditions of the model are shown in Figure 3. Three faces of the boundaries were considered as the viscous boundaries (non-reflecting) to eliminate the wave reflection.

The effect of changing the parameters on the stress changes in different parts of the model was investigated at 0.5 ms after the explosion. The position of these points is referred to each section.

The wave propagation mechanism in the basic state is shown in Figure 4. The stress changes in different conditions were compared by integrating the absolute value of stress in the stress-time diagram at each point. For example, the changes in the normal stress along the model x-axes for point J in Figure 5 follow the solid blue line in Figure 5. In this Figure, the horizontal axis and vertical axes represent the time changes and stress, respectively.

Taking the absolute value of the stress, the graph turns to the dashed yellow curve. The final number to check the state of stresses at each point is equal

to the integral below the graph. For example, the integral below the graph for point J will be 34000 Pa.s, according to Figure 4.

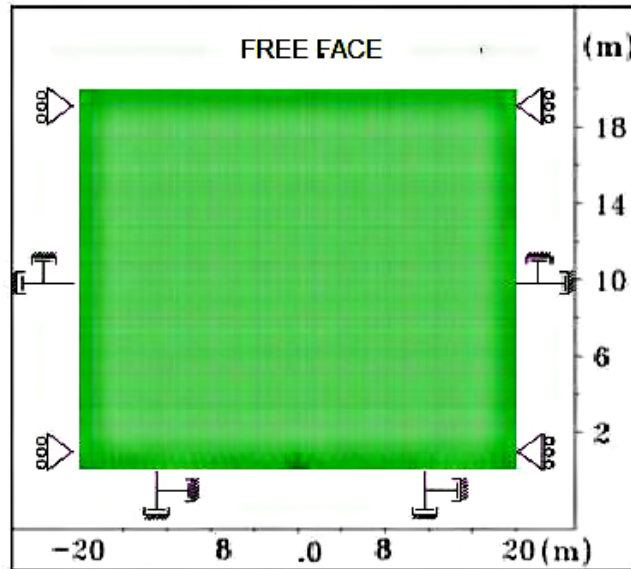


Figure 3. Boundary condition and geometry of the model.

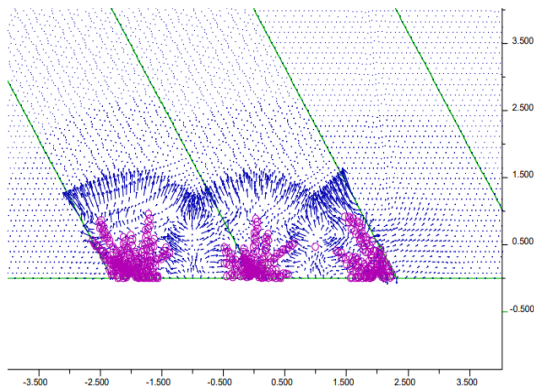


Figure 4. Wave propagation for the base model.

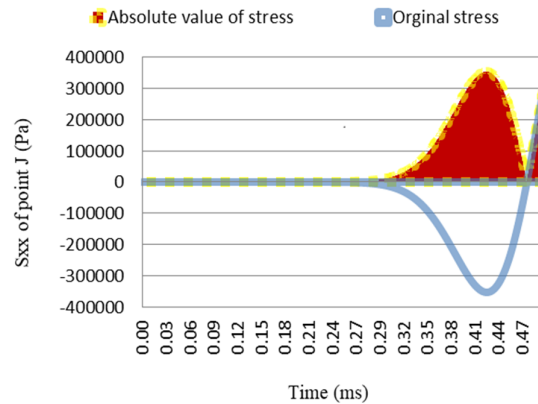
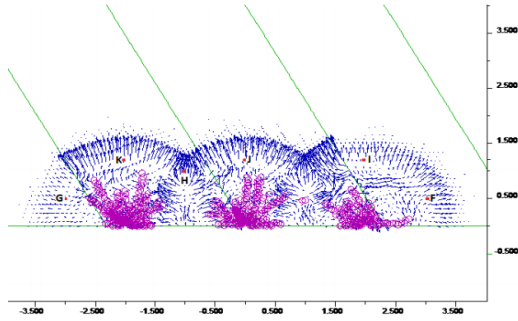


Figure 5. Original and absolute value stresses at point J.

### 3. Effect of geomechanical parameters of joints

The values for the joint parameters, joint normal stiffness (JKN), and shear stiffness (JKS) varied from 0.01 to 100 times the original value in Table 3. The effect of changes in these two parameters on the normal and shear stress changes was observed on six different points, as shown in Figure 6. In this Figure, the wave propagation inferred as JKN and

JKS is 10 times the base state (900 GPa/m for JKN). The mean stress level for the three points in front of the blast holes I, J, and K are as shown in Figure 7. In Figures 7 and 8, the x-axis and y-axis are the JKN-JKS changes and the integral of the absolute value of stress, respectively. This Figure shows that the stress increases with increasing the JKN and JKS values in general.



**Figure 6. Position of points F to K relative to the blast hole and wave propagation in the 10× JKN and 10 × JKS cases compared to the base state.**

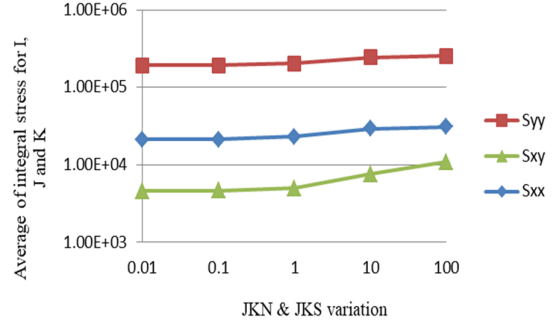
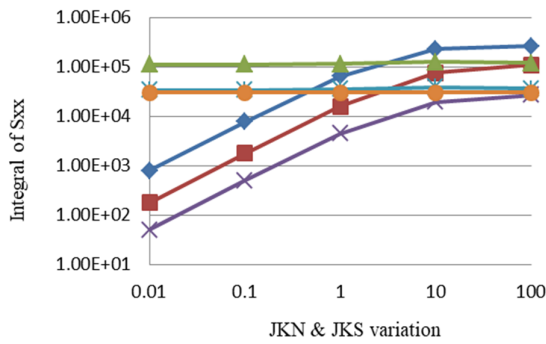


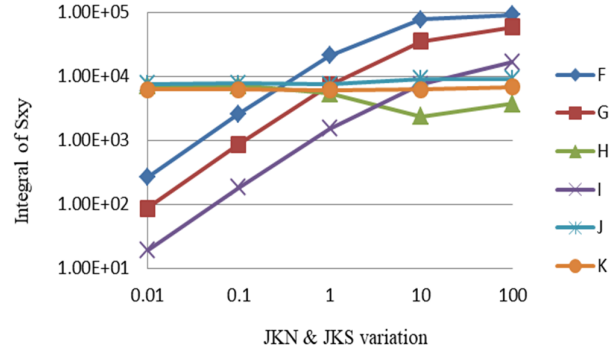
**Figure 7. Integral of mean stress at three points I, J, and K with JKN and JKS changes.**

As shown in Figure 8, in general, by increasing the values for JKN and JKS, the joint acts as a less effective barrier against the wave, and the blast behavior becomes closer to the rock without joint. The main difference between the three points G, I, and F and the three points H, J, and K is that there is a joint between G, I, and F and the location of the blast hole. The points H, J, and K indicate similar behaviors against the variations in JKN and JKS. The stress level for point H along with the directions

X and Y, due to closeness to the blast hole and placing between two boreholes, was higher than that between the points J and K. The amount of stress changes for the three points H, J, and K was negligible because there were no joints between the points to the blast hole. The stress changes for the three points G, I, and F are such that with increase in the joint strength, the amount of stress in these points is also increased.



(a)



(b)

**Figure 8. Stress changes for six points (F to K) due to changes in JKN and JKS relative to the base model.**

In order to analyze the influence of JKN and the influence of JKS in the extension of radial cracked and plastic zones around a blast hole, this analysis was done for a discontinuous medium with one joint, in which per section of this analysis, the geomechanical property of the joint was changed

(Figure 9). As depicted in Table 4, with a decrease in the JKN value, the radial cracked and plastic zones around a blast hole were increased more than the amount of plastic zones and radial cracks that were calculated from decrease in the JKS value.

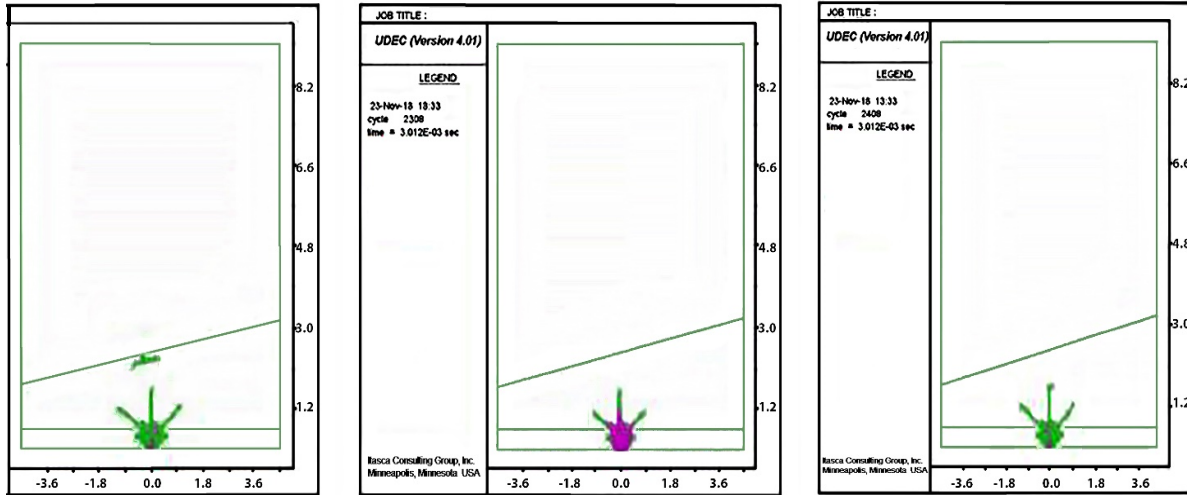


Figure 9. Influence of geomechanical joint parameter on plastic zone extension: a)  $jkn = 2e7$   $jks = 2e7$ , b)  $jkn = 2e11$   $jks = 2e7$ , c)  $jkn = 2e7$   $jks = 2e11$ .

Table 4. Overall result of geomechanical properties of joints in radial cracked and plastic zones.

JKN (Pa/m)	JKS (Pa/m)	Plastic zones (%)	Maximum of the radial cracked zone (m)
2e7	2e7	8.7	1.904
2e11	2e7	7.25	1.837
2e7	2e11	7.92	1.874

#### 4. Effect of geometrical parameters of joints

In this section, the geometrical parameters of joints such as the spacing, number and persistence that played an important role in the instability of the structures excavated in the rock were studied.

##### 4.1. Effect of joint spacing

In order to investigate the joint spacing, the amount of joint spacing was changed from 0.5 m to 4 m. The effect of spacing changes in the joint set was observed on six points. The position of these six points (F to K) was the same as that presented in Figure 6. Also the waveform for the mode with a distance of 1 m is as shown in Figure 10. Until 0.5 ms, with decrease in the joint spacing to 1 m, the impact on the wave direction is more sensible as in Figure 10 compared to Figure 4. The changes were greater when the joint spacing was less than the space between the blast holes (i.e. 2 m), and thereafter, a more constant trend occurred. As it can

be seen in Figure 11, these changes are also oscillating, increasing, and decreasing according to the position of the points, blast holes, and joints. The horizontal and vertical axes in Figures 11 and 12 represent the joint spacing and integral of the absolute value of stress, respectively.

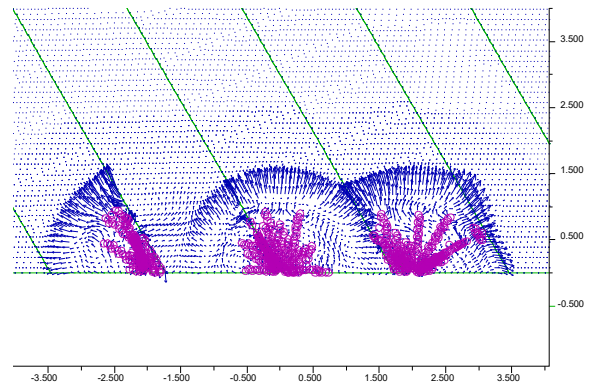


Figure 10. Wave propagation at a 1-m spacing of the joints from each other.

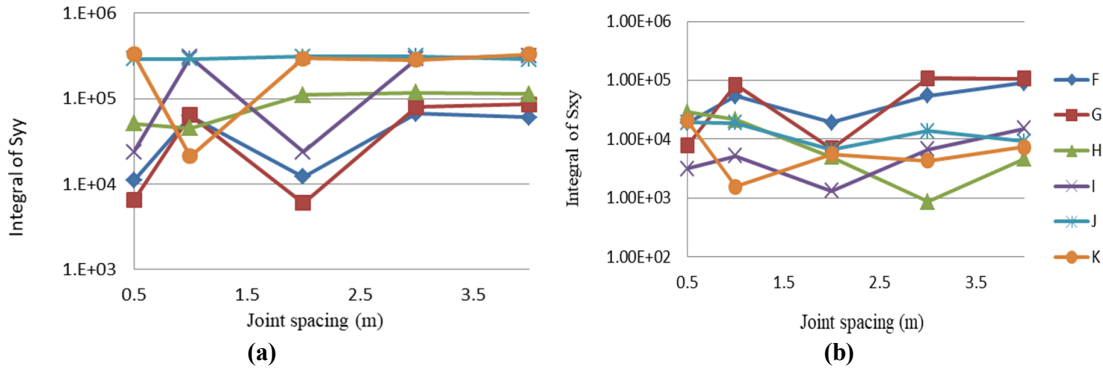


Figure 11. Stress changes for six points (F to K) due to changes in joint spacing relative to the base model.

The mean stress for the three points I, J, and K in front of the blast holes changed as shown in Figure 12. The stress values were the minimum for a 2-m spacing, which increased for a greater or smaller spacing. The normal and shear stresses had minimum values at distances of 1 m and 2 m, respectively. This indicates that by increasing the spacing relative to the distance of the blast holes and decreasing it, the rock mass has acted less inhomogeneously. Also most of the stress changes are related to increasing the distance from 2 m to 3 m.

4.2. Effect of joint angle with model x-axis

The joint set angle was changed simultaneously from  $60^\circ$  to  $180^\circ$  with a difference of  $30^\circ$  to  $60^\circ$  compared to the main value in the model. The effect of changes in the angle of the joint set is observed on six points. The position of these six points (F to K) is the same as in Figure 6. The direction of the waves according to the angle of the joint set was between the joints set, where each joint acted as a free surface against the wave (see Figure 13). There

is no change in the direction of wave motion for the joint angle vertical to the x-axis due to the equal distance between the blast hole and the joints (Figure 13(b)). The mean stress changes for the three points I, J, and K are presented in Figure 14. This figure shows the sinusoidal and repetitive stress changes according to the change in the joint angle. The x-axis and y-axis in Figures 14 and 15 are the joint angles and integral of the absolute value of stress, respectively.

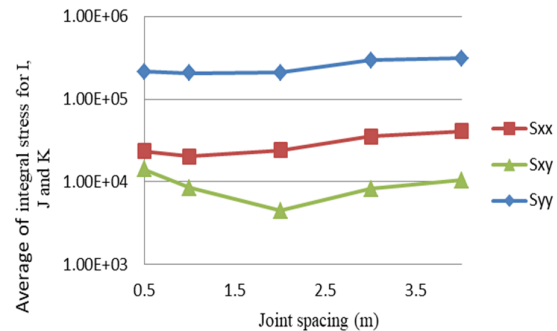


Figure 12. Integral of mean stress at three points I, J, and K with joint spacing changes.

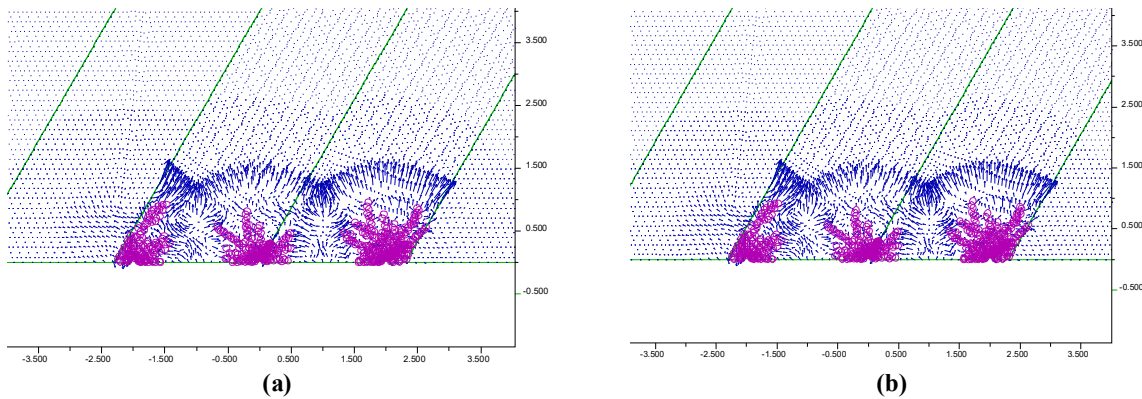


Figure 13. Wave propagation for joint angle with  $60^\circ$  (a) and  $90^\circ$  (b) joints, respectively.

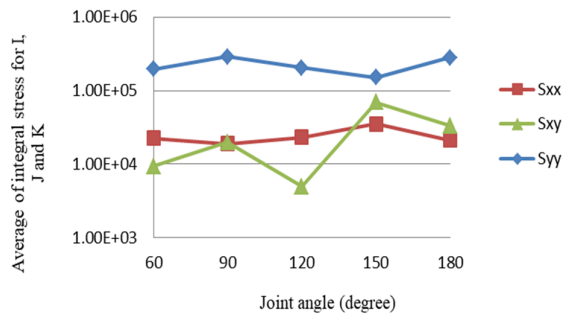


Figure 14. Integral of mean stress at three points I, J, and K with the joint angle with x-axis changes.

Variations in the conditions of the joint set angle depend on the location of the selected point (F to K) with respect to the blast hole and joints. In each step, with varying the joints tangle, the conditions of the target point vary versus the borehole and joints. The

mean variation is between 0° to 180° and in a sinusoidal form (Figure 14). The point-to-point study of these variations is discussed in the following. As it shown in Figure 15, the points F, G, and H, which were not selected in front of the blast holes, have a similar oscillating trend due to the angle changes. These changes are less for point H because it is located between the two blast holes. The least change in vertical stress is for point J because this point is in front of the top of the blast hole and the joint near it passes exactly over the middle blast hole. Point J is always subject to the same explosion even when the angle of the joints changes. The amount of horizontal stress changing at the two points I and K are parabolic. This can be attributed to the fact that by changing the angle, the horizontal stress moves from the middle blast hole toward the other side.

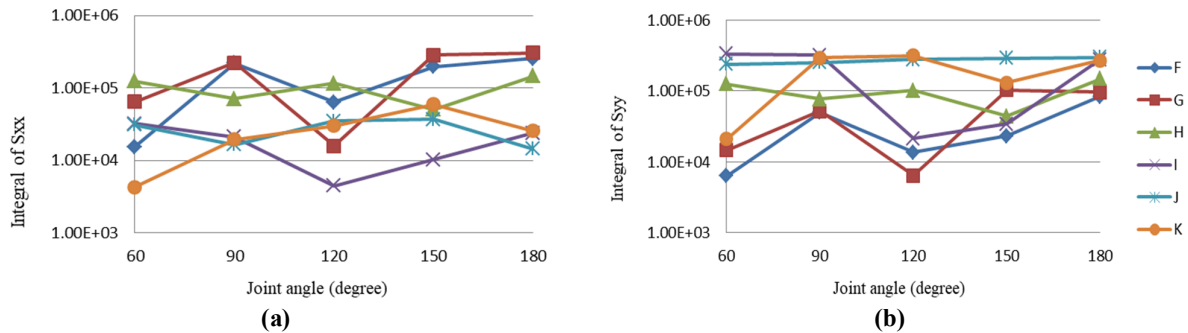


Figure 15. Stress changes for six points (F to K) due to changes in joint angle with the x-axis.

### 4.3. Effect of joint persistence on radial crack extension

The radial crack extension in a continuum medium, discontinuum medium with continuous persistence, and discontinuum medium with discontinuous persistence was analyzed, respectively. The geomechanical and geometrical properties are presented in Table 5.

In a continuum medium, as depicted in Figure 16(a), the maximum radial crack that happened was 1.49 m, which was located at 52.6° with respect to

the horizon direction and the number of zones that reached the plastic behavior, due to dynamic loading, was 252. In the discontinuum medium with continuous joint persistence, as depicted in Figure 16(b), the maximum of radial crack that happened was 1.264 m, which was located at 126° with respect to the horizontal direction, and the number of zones that reached the plastic behavior was 152.

Table 5. Geomechanical and geometrical properties of joint sets.

Joint set	Dip (°)	Spacing (m)	Jkn (Pa/m)	Jks (Pa/m)
1	32	0.5	2e7	2e7
2	72	0.5	2e7	2e7

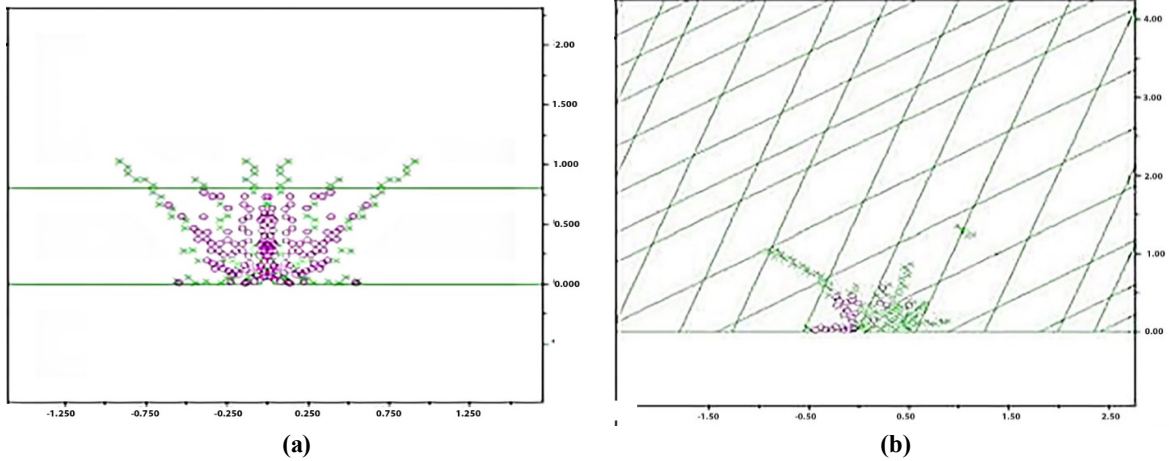


**Figure 16. Plastic and radial cracked zones around a hole because of blasting in continuum media (a) and discontinuum media with continuous joint persistence (b).**

In a discontinuum medium with discontinuous joint persistence (logical condition of the problem), as depicted in Figure 17, the maximum of radial crack that happened was 1.323 m, which was located at 88° with respect to the horizon direction, and the number of zones that reached the plastic zone due to dynamic loading was 200.

The compressive wave, which plays an important role in fracture growth around a blast hole for continuum (a) and discontinuum (b) joint persistence is depicted in Figure 18, respectively.

As shown in these Figures, the compressive wave transmission in continuous joint persistence, because of an extra joint persistence that defined the rock medium too weak was lower than the discontinuous joint persistence. Hence, the reflected compressive wave in continuous joint persistence was upper than discontinuous joint persistence. Hence, the crush zone, which was not a useful phenomenon in mining engineering was increased in the continuous joint persistence.

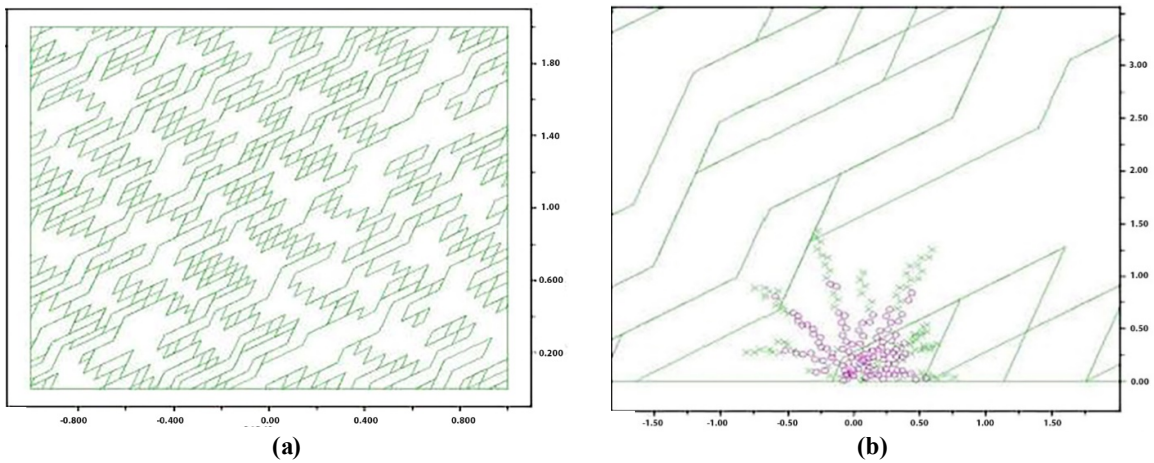


**Figure 17. Discontinuum medium with discontinuous joint persistence plastic zones and radial cracks around a hole.**

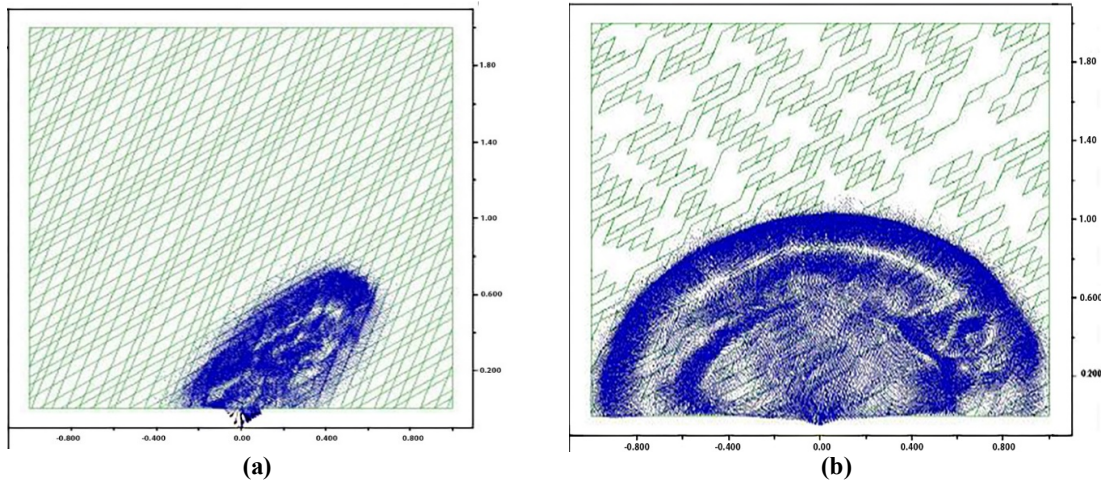


Figure 18. Compressive wave transmission in discontinuum medium with continuous joint persistence (a) and discontinuous joint persistence (b).

**5. Effect of geomechanical parameters of rock**

The values of the two parameters of shear modulus and bulk modulus changed simultaneously from 0.5 to 2 times the original value in the model. The effect of changes in these two parameters on the axial and shear stress changes was observed on six points. The position of these six points (F to K) with respect to the location of the blast holes is presented

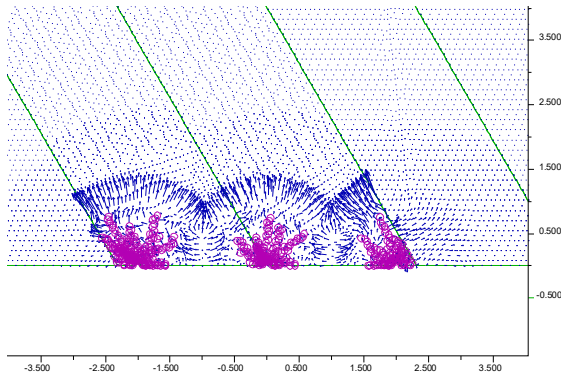


Figure 19. Wave propagation in half of shear and bulk modulus cases compared to the base state.

As shown in Figure 21, the rate of stress change decreased with increase in the shear modulus and bulk modulus. The stress will be less sensitive to the shear and bulk modulus more than the two blast holes, and no joint has separated this point to the

in Figure 6. Also wave propagation in the case where the bulk and shear moduli are half of the base model (5.56 and 4.17 GPa, respectively) is shown in Figure 19. In Figures 20 and 21, the x-axis and y-axis are the bulk and shear modulus changes and the integral of the absolute value of stress, respectively. The mean stress for the three points in front of the blast holes I, J, and K (Figure 20) increased with increase in the values of the bulk and shear modulus.

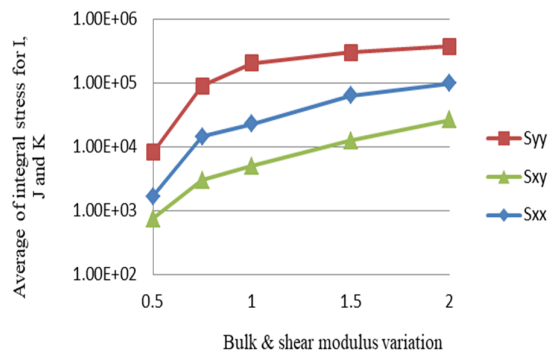


Figure 20. Integral of mean stress at three points I, J, and K with bulk and shear modulus changes.

location of the two blast holes. The effect of changing the amount of shear modulus and bulk desblast hole smaller changes (0.5 to 2 times) was more than the effect of JKN and JKS (0.01 to 100 times) on the explosion.

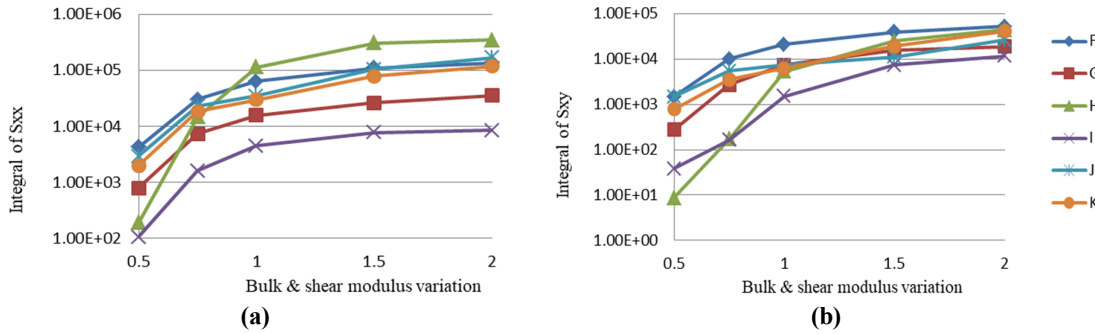


Figure 21. Stress changes for six points (F to K) due to changes in bulk and shear modulus relative to the base model.

The effect of the rock density change on the mean stress of the three points in front of the blast holes is presented in Figure 22. As it can be seen, the amount of stress decreases gently with increase in the rock density, and less energy will reach the points around the blast hole. The effect of density on stress is less than the other factors investigated so far.

6. Effect of blast hole spacing

The distance between the blast holes was changed from 1 m to 4 m. The wave propagation in the 1-meter spacing of the blast holes can be seen in Figure 23. The effect of changing the distance of the holes was observed on five points with different arrangements than the previous cases. The position of the stress change monitoring points was selected so that they had the same definition in different spacings. In all cases, the vertical distance to the measuring point was 1.5 m, the points G and I were

between the two blast holes, point H was in front of the middle blast hole, and the two points J and F were 0.5 m away from the two-side blast holes. The position of these five points (F to J) for a 1-m spacing of the holes is as shown in Figure 23.

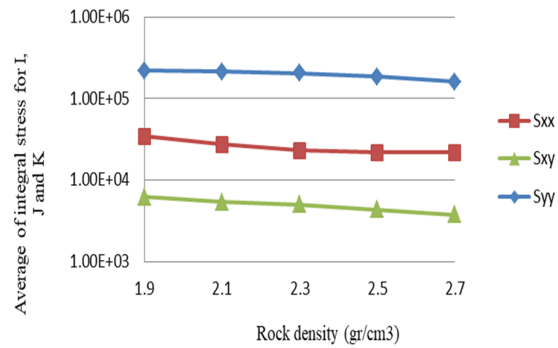


Figure 22. Integral of mean stress at the three points I, J, and K with density changes.

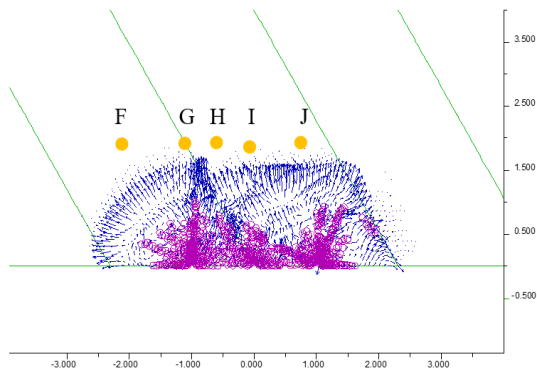


Figure 23. Wave propagation for 1-m blast hole spacing.

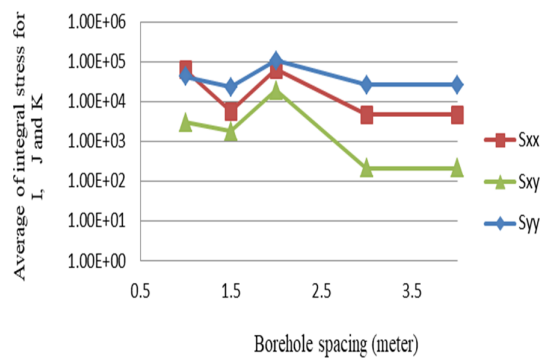
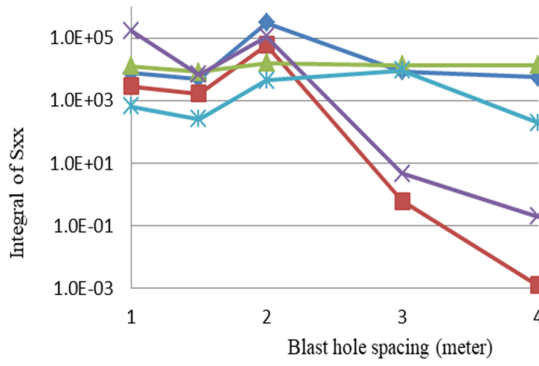


Figure 24. Integral of mean stress at three points I, J, and K with blast hole spacing changes.

According to Figure 24, the maximum amount of stress was obtained at 2 m distance of blast holes from each other. In general, it can be stated that the best explosion mode with these conditions is 2-m spacing. Therefore, from Figure 25, it can be stated

that with respect to the joint set angles, for spacings less than 2 m, point J has a distance of one joint from the blast hole and has a less stress compared to the other points. However, with increasing the blast hole spacing to more than 2 m, the amount of stress

at two points between the two blast holes (G and I) decreased sharply. The x-axis and y-axis in Figures



24 and 25 are the borehole spacing and the integral of the absolute value of stress, respectively.

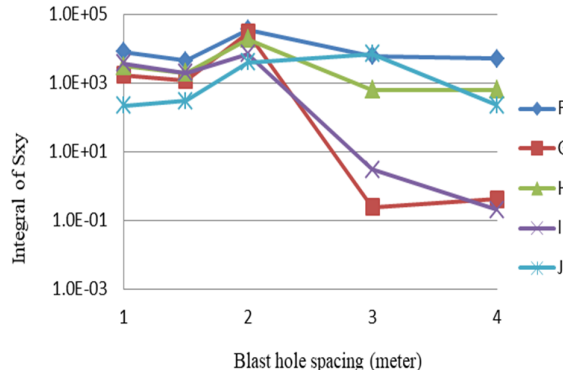


Figure 25. Stress changes for five points (F to J) due to changes in blast hole spacing.

7. Conclusions

In this work, we used the UDEC software to model the blast hole explosion in jointed rock mass in order to investigate the influence of the geomechanical and geometrical properties on the stress distribution and radial crack extension. The critical parameters analyzed for this aim included the normal stiffness (JKN) and shear stiffness (JKS), spacing, angle and persistence of joint, shear and bulk modulus, density of rock, and borehole spacing.

It was obtained that with increase in the joint strength, the stress level in the points, which were also affected by a joint, was increased. The results obtained showed that stress increased with the increasing JKN and JKS values, in general. Also with decrease in the JKN and JKS values, the radial cracked and plastic zones around a blast hole showed more development. Stress changes by joint spacing were also oscillating, increasing, and decreasing according to the position of the point, blast hole, and joint. The direction of the waves according to the angle of the joint set was between the joints set, where each joint acted as a free surface against the wave. The simulation shows the sinusoidal and repetitive stress changes according to the change in the joint angle.

With increase in the joint persistence, plastic zones decreased around a blast hole. Hence, the crush zone around a blast hole, due to an increase in a reflected wave, was expanded and the amount of maximum radial crack was decreased. The wave transmission in the continuous joint was lower than that for the discontinuous joint. The reason is that a higher joint persistence makes the rock medium too weak. The mean stress for the three points in front of the blast holes I, J, and K increased significantly

with increase in the values of the bulk and shear modulus. The amount of stress decreases gently with increasing rock density. The maximum amount of stress was obtained at a 2-m distance of blast holes from each other, and the best mode of explosion with these conditions was a 2-m spacing.

Rock mass blasting is a function of variations factors, and their design can provide the best blasting pattern. In this work, the effects of some of these factors on blasting were investigated. However, studying blasting in a wider time horizon can provide better results. Moreover, the 3D modelling of blasting allows a better understanding of the effect of joint slope and wave propagation.

References

[1]. Cai, J. G. and Zhao, J. (2000). Effects of multiple parallel fractures on apparent attenuation of stress waves in rock masses. *International Journal of Rock Mechanics and Mining Sciences*. 37 (4). 661-682.

[2]. Jimeno, E.L., Jimino, C.L. and Carcedo, A. (1995). *Drilling and blasting of rocks*. CRC Press.

[3]. Zhu, F., Dui, G. and Ren, Q. (2011). A continuum model of jointed rock masses based on micromechanics and its integration algorithm. *Science China Technological Sciences*. 54 (3). 581-590.

[4]. Zhang, Q. B. and Zhao, J. (2014). A review of dynamic experimental techniques and mechanical behaviour of rock materials. *Rock mechanics and rock engineering*. 47 (4). 1411-1478.

[5]. Norouzi Masir, R., Ataei, M. and Mottahedi, A. (2020). Risk assessment of flyrock in surface mines using FFTA-MCDMs combination. *Journal of Mining and Environment*.

[6]. Sharpe, J.A. (1942). The production of elastic waves by explosion pressures. I. Theory and empirical field

observations. *Geophysics*. 7 (2). 144-154.

[7]. Konya, C.J. and Walter, E.J. (1991). Rock blasting and overbreak control (No. FHWA-HI-92-001; NHI-13211). United States. Federal Highway Administration.

[8]. Koopialipoor, M., Fallah, A., Armaghani, D.J., Azizi, A. and Mohamad, E.T. (2019). Three hybrid intelligent models in estimating flyrock distance resulting from blasting. *Engineering with Computers*. 35 (1). 243-256.

[9]. Cho, S.H., Nakamura, Y. and Kaneko, K. (2004). Dynamic fracture process analysis of rock subjected to stress wave and gas pressurization. *International Journal of Rock Mechanics and Mining Sciences*. 41. 433-440.

[10]. R.L. Ash, "Mechanics of rock breakage; material properties, powder factor, blasting costs," *Pit Quarr*. 1963, pp. 109-111, 1963.

[11]. Drukovanyi, M.F., Komir, V.M., Myachina, N.I., Rodak, S.N. and Semenyuk, E.A. (1973). Effect of the charge diameter and type of explosive on the size of the overcrushing zone during an explosion. *Soviet Mining*. 9 (5). 500-506.

[12]. Vovk, A. A., Mikhalyuk, A. V. and Belinskii, I.V. (1973). Development of fracture zones in rocks during camouflet blasting. *Soviet Mining*. 9 (4). 383-387.

[13]. Szuladzinski, G. (1993). Response of rock medium to explosive borehole pressure. In *International symposium on rock fragmentation by blasting* (pp. 17-23).

[14]. Kanchibotla, S.S., Valery, W. and Morrell, S. (1999, November). Modelling fines in blast fragmentation and its impact on crushing and grinding. In *Explo '99—A conference on rock breaking*, The Australasian Institute of Mining and Metallurgy, Kalgoorlie, Australia (pp. 137-144).

[15]. Esen, S., Onederra, I. and Bilgin, H.A. (2003). Modelling the size of the crushed zone around a blasthole. *International Journal of Rock Mechanics and Mining Sciences*. 40 (4). 485-495.

[16]. Iverson, S.R., Hustrulid, W.A., Johnson, J.C., Tesarik, D. and Akbarzadeh, Y. (2009, September). The

extent of blast damage from a fully coupled explosive charge. In *Proceedings of the 9th International Symposium on Rock Fragmentation by Blasting, Fragblast* (Vol. 9, pp. 459-68).

[17]. Siamaki, A. and Bakhshandeh Amnieh, H. (2016). Numerical analysis of energy transmission through discontinuities and fillings in Kangir Dam. *Journal of Mining and Environment*. 7 (2). 251-259.

[18]. Ma, G.W. and An, X.M. (2008). Numerical simulation of blasting-induced rock fractures. *International Journal of Rock Mechanics and Mining Sciences*. 45 (6). 966-975.

[19]. Cundall, P.A. (1990). Numerical modelling of jointed and faulted rock. In *International conference on mechanics of jointed and faulted rock* (pp. 11-18).

[20]. Sharafisafa, M., Aliabadian, Z., Alizadeh, R. and Mortazavi, A. (2014). Distinct element modelling of fracture plan control in continuum and jointed rock mass in presplitting method of surface mining. *International Journal of Mining Science and Technology*. 24 (6). 871-881.

[21]. Kulatilake, P.H., Shreedharan, S., Sherzadeh, T., Shu, B., Xing, Y. and He, P. (2016). Laboratory estimation of rock joint stiffness and frictional parameters. *Geotechnical and Geological Engineering*. 34 (6). 1723-1735.

[22]. Wang, Z.L. and Konietzky, H. (2009). Modelling of blast-induced fractures in jointed rock masses. *Engineering Fracture Mechanics*. 76 (12). 1945-1955.

[23]. Wang, Z.L., Li, Y.C. and Wang, J.G. (2008). Numerical analysis of blast-induced wave propagation and spalling damage in a rock plate. *International Journal of Rock Mechanics and Mining Sciences*. 45 (4). 600-608.

[24]. Wang, Z. L., Li, Y. C., & Shen, R. F. (2007). Numerical simulation of tensile damage and blast crater in brittle rock due to underground explosion. *International Journal of Rock Mechanics and Mining Sciences*. 44 (5). 730-738.

## آنالیز حساسیت تنش و رشد ترک در آتشباری توده سنگ با استفاده از مدلسازی عددی

محمدعلی چمن‌زاد و مجید نیکخواه\*

دانشکده مهندسی معدن، نفت و ژئوفیزیک، دانشگاه صنعتی شاهرود، ایران

ارسال ۲۰۲۰/۰۸/۳۱، پذیرش ۲۰۲۰/۰۹/۲۱

\* نویسنده مسئول مکاتبات: m.nikkhah@shahroodut.ac.ir

### چکیده:

حفاری و آتشباری یکی از موارد پرکاربرد در رشته‌های مهندسی عمران و معدن است. آنالیز رفتار چالزنی و آتشباری به سبب دو عامل اصلی تشکیل دهنده توده سنگ، ماتریکس سنگ بکر و درزه‌ها، با پیچیدگی‌هایی همراه است. هدف از تحقیق پیش‌رو، بررسی اثر پارامترهای ژئومکانیکی و هندسی سنگ و ناپیوستگی‌ها بر روی آتشباری با استفاده از نرم افزار UDEC است. به همین منظور از کد دوبعدی المان مجزا استفاده شده است تا شبیه سازی تنش در اطراف سه چال آتشباری و گسترش ترک شعاعی ناشی از آتشباری بررسی شود. پارامترهای مورد بررسی شامل سختی نرمال و برشی، فاصله داری، پایداری و زاویه دسته درزه، مدول بالک و برشی و چگالی سنگ و فاصله داری چاه‌ها است. نتایج نشان می‌دهند که پارامترهای مرتبط با درزه و مدول سنگ بیشترین تاثیر را دارند و در حالی که چگالی سنگ کمترین تاثیر را در بین این پارامترها دارد. همچنین مقدار تنش با سختی برشی، نرمال، مدول بالک و برشی رابطه مستقیم و با چگالی سنگ رابطه معکوس دارد. تغییرات تنش با توجه به فاصله داری و زاویه دسته درزه به صورت سینوسی و تکرار شونده با توجه به موقعیت نقطه هدف، چال انفجار و دسته درزه تغییر می‌کند. زون ترک شعاعی و پلاستیک در اطراف چال انفجار با کاهش سختی برشی و نرمال درزه‌ها گسترش بیشتری یافته است. با افزایش پایداری دسته درزه زون پلاستیک اطراف چال انفجاری کاهش یافته است.

**کلمات کلیدی:** آتشباری، روش المان مجزا، مدلسازی عددی، ناپیوستگی، توده سنگ.